 DOI: 10.1002/masy.200900080

Study of the Morphology Exhibited by Linear Segmented Polyurethanes

Iaci Miranda Pereira,[1,2] *Rodrigo Lambert Oréfice*[*2]

Summary: Five series of segmented polyurethanes with different hard segment content were prepared by the prepolymer mixing method. The nano-morphology of the obtained polyurethanes and their microphase separation were investigated by infrared spectroscopy (FTIR), modulated differential scanning calorimetry (MDSC) and small-angle X-ray scattering (SAXS). Although highly hydrogen bonded segments were formed, high hard segment contents led to the presence of elevated degree of phase mixture and reduced the chain mobility, decreasing the hard domain precipitation and the soft segment crystallization. The applied techniques were able to show that the hard-segment content and the hard-segment interactions were the two controlling factors for determining the structure of segmented polyurethanes.

Keywords: microphase separation; nano-morphology; polyurethanes; SAXS

Introduction

Segmented polyurethanes (PUs) are multiblock copolymers which consist of the so-called hard and soft segments. The multiphase structure of PUs results from the repulsive interaction between dissimilar segments and thermodynamic immiscibility of hard and soft segments at low temperature. The microphase separation structure of PUs depends on many factors, including structure and molecular weight of the soft segment, nature of chain extender, hard segment content and interactions, thermal and solvent history during sample preparation.[1–4] In the present work, PUs were synthesized in an aqueous environment by combining hard segments derived from aliphatic isophorone diisocyanate with soft segments based on poly(caprolactone diol). Five series of PUs having different hard segment contents were synthesized. The infrared spectroscopy (FTIR), modulated differential scanning calorimetry (MDSC) and small-angle X-ray scattering (SAXS) were used to provide information about the nano-morphology of the obtained PUs and on their microphase separation.

Materials and Methods

Polymer Synthesis

Poly(caprolactone diol) (PCL – Mn = 530, 1250, 2000, 10000 g mol^{-1} – values informed by supplier), isophorone diisocyanate (IPDI), 2,2-bis(hydroxymethyl) propionic acid (DMPA) and dibutyl tin dilaurate (DBDLT) were obtained from Aldrich (St. Louis, MO). Triethylamine (TEA, 98%) and hydrazine (HZ, 25%) were purchased from Vetec (RJ, Brazil). All these chemicals were employed throughout this work without any previous treatment. PUs were prepared by the prepolymer mixing method, according to a procedure that will be described in previous work.[5] The feed ratios are shown in Table 1, where $W(HS)$ is weight fraction of hard segment content,

[1] Federal Center of Technological Education of Minas Gerais, Av. Amazonas 1193, Vale Verde, Timóteo, Minas Gerais, Brazil, 35.183-006
[2] Federal University of Minas Gerais, Department of Metallurgical and Materials Engineering, Rua Espírito Santo 35, Centro, Belo Horizonte, Minas Gerais, Brazil, 30160-030
E-mail: rorefice@demet.ufmg.br

Table 1.
Composition (wt.%) of waterborne PUs.

	PCL				DMPA	IPDI	HZ	TEA	$W(HS)$
	530	1250	2000	10000					
PU530	34.3	–	–	–	6.6	50.5	3.6	4.9	57.0
PU1250	–	55.4	–	–	4.5	34.6	2.1	3.4	38.0
PU2000	–	–	66.1	–	3.3	25.8	1.9	3.0	28.5
PU10000&530	7.1	–	–	72.0	2.1	16.1	1.2	1.6	17.5
PU10000	–	–	–	90.8	0.9	7.1	0.5	0.7	7.6

obtained according to Equation 1.

$$W(HS) = \frac{Weight_{IPDI} + Weight_{HZ}}{Weight_{PU}} \times 100 \quad (1)$$

Infrared Spectroscopy

Infrared spectra were collected in a Fourier transform infrared spectrophotometer (FTIR; Perkin–Elmer, model Spectrum 1000). Measurements were carried out using the attenuated total reflectance (ATR) technique. Each spectrum was a result of 64 scans with a resolution of $4\,cm^{-1}$.

Modulated Differential Scanning Calorimetry (MDSC)

MDSC measurements were performed using a TA Instruments 2920. The following protocol was applied to each sample: (1) heating from room temperature to 110 °C at 15 °C min^{-1}, (2) holding for 3.00 min at 110 °C, (3) cooling to −110 °C at 3.00 °C/min, modulating +/− 1.00 °C every 60 s. The glass transition temperatures (T_g) were obtained by the analysis software of the calorimeter.

Synchrotron Small Angle X-Ray Scattering (SAXS)

SAXS measurements of synchrotron small angle X-ray scattering were performed using the beam line of the National Synchrotron Light Laboratory (LNLS, Campinas, Brazil). After passing through a thin beryllium window, the beam was monochromatized ($\lambda = 1.488$ Å) and horizontally focused by a cylindrically bent and asymmetrically cut silicon single crystal. The X-ray scattering intensity, $I_{(q)}$, was experimentally determined as a function of the scattering vector, q, whose modulus is given by Equation 2:

$$q = \frac{4\pi}{\lambda}\sin\theta \quad (2)$$

where λ is the X-ray wavelength and θ represents half the scattering angle.

Each SAXS pattern corresponded to a data collection time of 900 s. From the experimental scattering intensity produced by all the studied samples, the parasitic scattering intensity produced by the collimating slits was subtracted. All SAXS patterns were corrected for the non-constant sensitivity of the position sensitive X-ray detector, for the time-varying intensity of the direct synchrotron beam and for differences in sample thickness. Because of the normalization procedure, the SAXS intensity was determined for all samples in the same arbitrary units so that they could be directly compared. The sample-detector distance of 551.6 mm was used during the measurements. The samples dimensions were 5 mm × 5 mm × 1 mm.

Results and Discussion

Typical infrared spectra of obtained PUs are shown in Figure 1. As shown, the position of the absorption bands of each specific functional group was similar for all obtained PUs.

The primary amine stretching modes appear at 3600–3150 cm^{-1}. The absorption band at about ~3300 cm^{-1} corresponds to hydrogen bonded −N−H group and absorption at ~3500 cm^{-1} to nonbonded

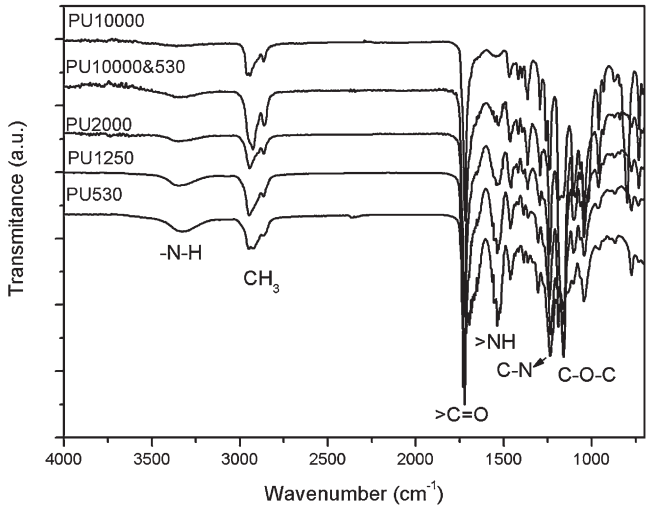

Figure 1.
FTIR spectra of PU530, PU1250, PU2000, PU10000&530 and PU10000 samples.

–N–H. The carbonyl group stretching vibrations, C=O, appear at 1760–1600 cm^{-1}. A series of specific absorption bands are present within the 1760–1600 cm^{-1} broad band, such as the absorption band due to the ester bond from PCL soft segments and others associated with multiple interactions between urea and urethane bonds and –N–H groups. IR bands at ~1720 cm^{-1}, ~1700 cm^{-1}, ~1660 cm^{-1}, ~1630 cm^{-1} are assigned, respectively, to free urethane stretching band, hydrogen bonded urethane stretching band, free urea stretching band and hydrogen bonded urea stretching band. The secondary amide absorption, >N–H, appears at 1640–1540 cm^{-1}. The band at 1150 cm^{-1} is assigned to the stretching of the –C–O–C– group.[5]

Hydrogen bonding is known as an important driving force for the phase separation of a hard segment from a soft-segment matrix. Thus, the carbonyl region has generally been investigated for the quantitative study of microphase separation or mixing in PU.[6] However, two main spectral regions are of interest in studying the hydrogen bonding of segmented PUs: N–H and C=O, respectively, primary amine stretching and carbonyl group stretching. Since band overlapping is observed, a deconvolution mathematical procedure (using the PickFiT® software) was performed on spectra of Figure 1 to enhance resolution of each individual band.

The extent of the –NH groups participating in hydrogen bonding can be expressed by a (–NH) hydrogen-bonding index $HBI^{(\%)}_{(-NH)}$, Equation 3.

$$HBI^{(\%)}_{(-NH)} = \frac{NH_{Bonded}}{NH_{Bonded} + NH_{Free}} \times 100 \quad (3)$$

where NH_{Bonded} and NH_{Free} are respectively the band peak area of bonded and free –NH groups.

The extent of the carbonyl absorption groups participating in hydrogen bonding can be expressed by a hydrogen-bonding index $HBI^{(\%)}_{(C=O)}$, which is the fraction of hydrogen bonded in the carbonyl groups stretching vibrations Equation 4.[7–9]

$$HBI^{(\%)}_{(C=O)} = \frac{A_{1700} + A_{1640}}{A_{1700} + A_{1640} + A_{1724} + A_{1660}} \quad (4)$$

where A_{1724}, A_{1700}, A_{1660}, and A_{1640} are respectively the band peak area of free urethane, bonded urethane, free urea, bonded urea and ester.

The degree of phase mixture, $DPM(\%)$, can be calculated from the fraction of hard segment dissolved in soft domain,

Table 2.
FTIR results of as-molded poly(ester–urethanes).

	$HBI^{(\%)}_{(-NH)}$	$HBI^{(\%)}_{(C=O)}$	α_{FTIR}	DPM (%)
PU530	96.21	54.24	0.000	37.73
PU1250	98.95	46.27	6.77	24.76
PU2000	94.40	54.74	29.14	15.25
PU10000&530	85.38	46.55	41.57	10.17
PU10000	63.65	31.78	54.78	5.35

Equation 5.[7] Results are summarized in Table 2.

$$DPM(\%) = \frac{\left(1-HBI^{(\%)}_{(C=O)}\right) \times W(HS)}{\left(1-HBI^{(\%)}_{(C=O)}\right) \times W(HS) + (1-W(HS))} \quad (5)$$

The IR bands at $1160\,cm^{-1}$ and $1190\,cm^{-1}$ in Figure 1 are associated, respectively, with C–O amorphous and crystalline bands. As band overlapping also occurs, deconvolution procedures were performed. The separated curves are shown in Figure 2. The FTIR crystallinity index, α_{FTIR}, was defined according to Equation 6:

$$\alpha_{FTIR} = \frac{A_{1190}}{A_{1190} + A_{1160}} \times 100 \quad (6)$$

where A_{1190} and A_{1160} are respectively the band peak area of C–O amorphous and crystalline band.

Figure 2 illustrates the deconvolution procedure used to determine the overlapped

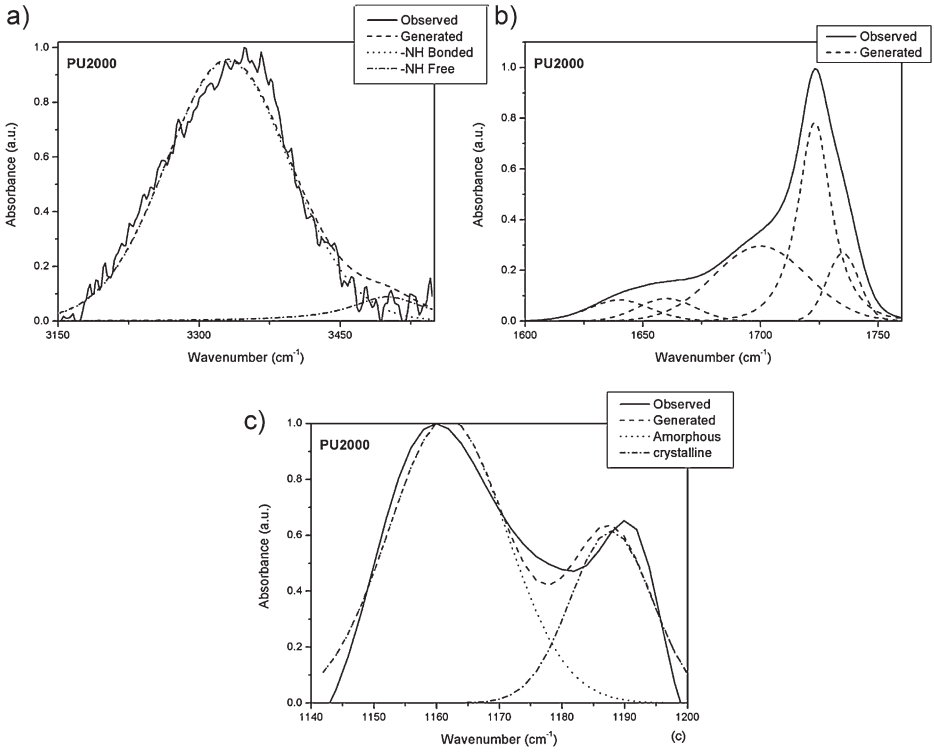

Figure 2.
Illustration of the deconvolution procedure used to determine the overlapped band of FTIR spectrum: (a) primary amine stretching, (b) carbonyl group stretching and (c) ether stretching.

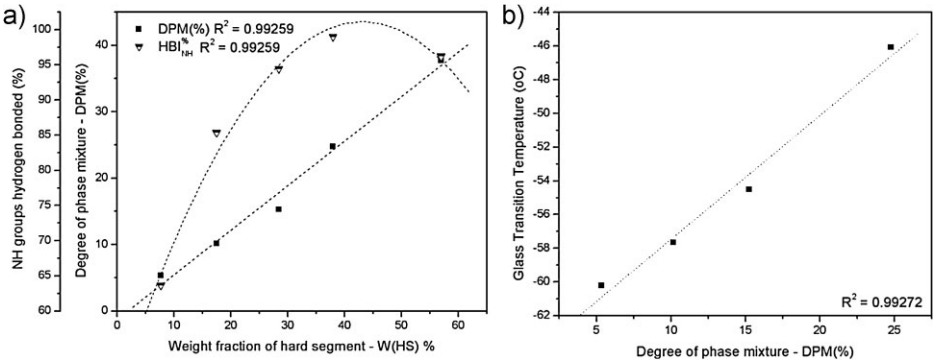

Figure 3.
(a) Influence of hard segment content on degree of phase mixture and (b) influence of the hard segment on glass transition.

band of FTIR spectrum of obtained PUs. Results are summarized in Table 2.

The multi-phase structure of PUs is a result of the repulsive interaction between dissimilar segments and thermodynamic immiscibility of hard and soft segments at low temperature.[1–3]

A linear relationship between hard segment content and $DPM(\%)$was observed, Figure 3(a). PUs having high hard segment, i.e. PU530, contents were produced by using low molar mass PCL oligomers that display higher levels of chain mobility. This enhanced mobility can be useful in allowing urethane and urea groups to align themselves to form hydrogen bonds. The highly hydrogen bonded hard segments act as physical cross-links, restricting segmental motion of the polymer chain. However, it does not result in a more significant phase separation between hard and soft segments because the weight fraction of hard segment. On the other hand, the lower values of $HBI(\%)$ of PU10000 do not result in a more extensive phase mixing since the reduction in hydrogen bonding within hard segments was compensated by an increase in the amount of soft segments. The hard segment content controls also the total of NH groups hydrogen bonded, Figure 3(a).

Thermal properties are summarized in Table 3. The second order transition, T_g, is observed around $-60\,^{\circ}C$. In DSC analysis, the width of transition zone provides a qualitative measure of phase homogeneity, and the variation in the magnitude of T_g can indicate the degree of microphase separation.[10] Higher degree of hard segment dissolved in the soft segment delays the phase transition moving T_g to higher values, Figure 3(b).

Figure 4 illustrates SAXS 2D pattern of the obtained PUs. The patterns and intensity distribution of SAXS are dependent on the shape, the size and size distribution of scattering objects.[11] Different nano-morphologies are observable, varying from one phase system to multiphase polymers. Differences in electron density of phases that fluctuate from a low phase density to highly packed structures are responsible for the observed scattering pattern.

Table 3.
DSC results of obtained poly(ester urethane).

	T_g (°C)	T_{onset} (°C)	T_{end} (°C)	Zone width
PU1250	−46.09	−53.80	−33.58	20.22
PU2000	−54.51	−59.65	−46.45	13.20
PU10000&530	−57.66	−64.65	−45.53	19.12
PU10000	−60.22	−64.09	−53.09	11.00

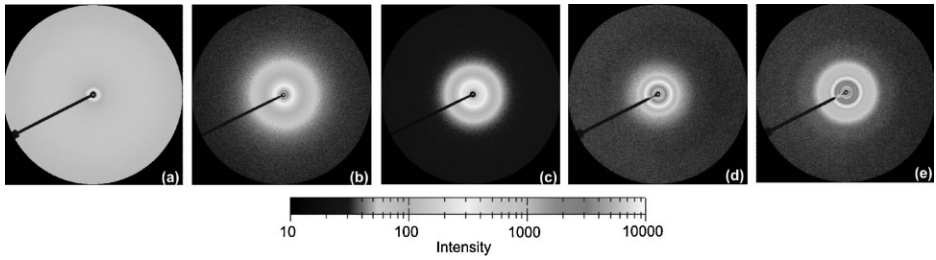

Figure 4.
SAXS pattern of: (a) PU530, (b) PU1250, (c) PU2000, (d) PU10000&530 and (e) PU10000.

Figure 5(a) illustrates SAXS data of the obtained PUs. The scattering peak observed in SAXS data of PU2000, PU10000&530 and PU10000 arises due to local heterogeneities in the electron density of the materials and it is usually interpreted as a consequence of the presence of distinct microphases with different electronic densities. However, to discuss the phase separation, it is convenient to employ the Lorentz correction, Q_{inv}, which describes the electron density fluctuation of polymer and is a good approximation to estimate the overall degree of phase separation in segmented polymers, Figure 5(b).[11–12] The Lorentz correction, the invariant quantity, Q_{inv}, can be obtained by integrating $I_{(q)}q^2$ over the range of scattering angles, Equation 7.[11–12]

$$Q_{inv} = \int_0^\infty I_{(q)}q^2 dq \qquad (7)$$

where $I_{(q)}$ is X-ray scattering intensity and q the scattering vector.

PU530 profile decreases monotonically with q, implying a high degree of phase mixture. The system can be thought as one phase structure. PU1250, PU2000, PU10000&530 and PU10000 present a multiphase structure including: amorphous matrix, hard domains and crystals. The contribution of each phase to the Lorentz corrected SAXS patterns were separated by a deconvolution procedure, Figure 6.[11-12]

Q_{inv} of each phase was obtained as fraction of the total area. The morphology of the polymer was investigated through the inter-domain repeat distance, L_{domain}, and/or lamellar crystalline repeat distance, $L_{Crystal}$. L is estimated from the q_{max} corresponding to the maximum of $I_{(q)}q^2$ versus q curves using Bragg's equation, Eq. 8.[11–12] Table 4 summarizes the results.

$$L = \frac{2\pi}{q_{max}} \qquad (8)$$

Since Q_{inv} is obtained by integrating $I_{(q)}q^2$ over the range of scattering angles,

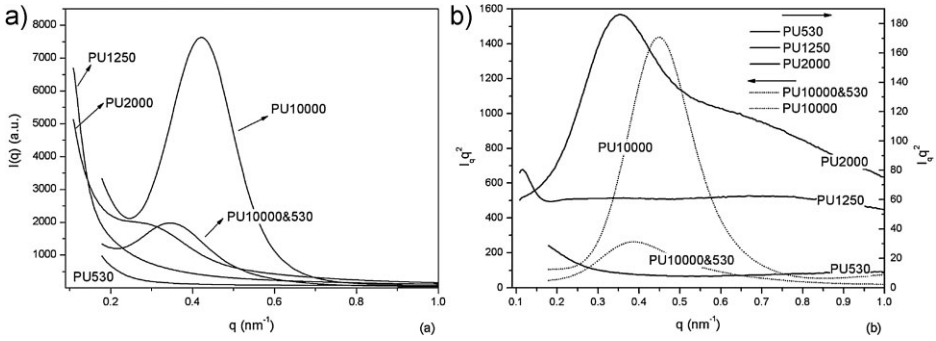

Figure 5.
(a) SAXS curves of obtained PUs and (b) Deconvoluted Lorentz SAXS pattern of samples.

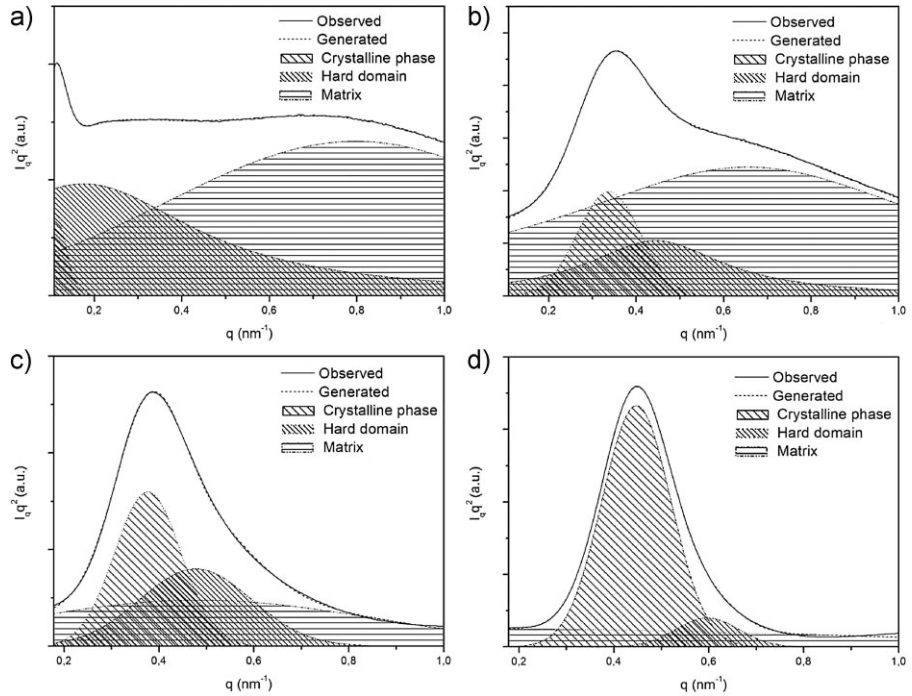

Figure 6.
Deconvoluted Lorentz SAXS patterns: (a) PU1250, (b) PU2000, (c) PU10000&530 and (d) PU10000.

phases with higher electron densities like crystals achieve higher integrated values. As indicated by α_{FTIR} and SAXS's crystalline phase, PU10000&530 is more crystalline than PU2000, hence one should expected higher integrated values for PU10000&530 than PU2000. However, this is not observed, possibly because the presence of PCL530 in soft segments of PU10000&530 would restrict chain packing efficiency, resulting in the formation of a less perfectly crystal structure.

SAXS and FTIR results show a good correlation. Q_{inv} describes the overall

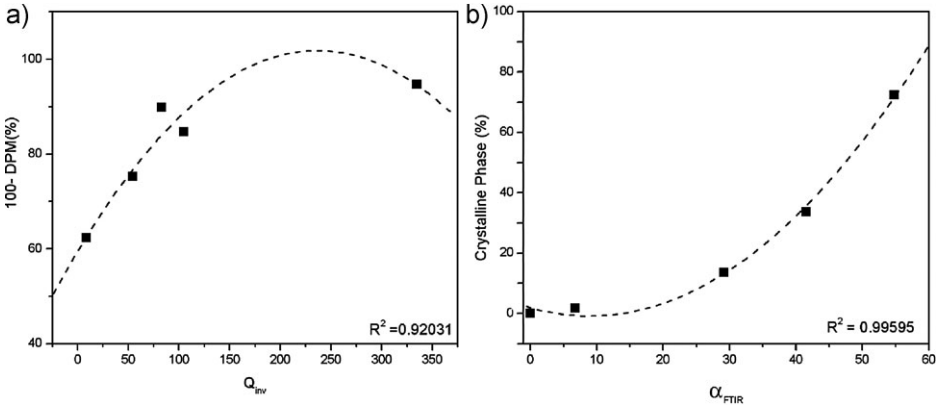

Figure 7.
Correlation between SAXS and FTIR results.

Table 4.
Deconvoluted SAXS results of crystalline phase, hard domains and matrix.

	Q_{inv}	Q_{inv}(%)			L (nm)	
		Crystalline phase	Hard Domain	Matrix	$L_{Crystal}$	L_{domain}
PU530	8.72	–	–	100.00	–	–
PU1250	54.48	1.72	31.48	66.80	55.30	35.97
PU2000	104.95	13.53	17.50	68.96	18.57	14.17
PU10000&530	82.83	33.70	28.25	38.05	16.69	13.17
PU10000	334.85	72.37	7.93	19.70	14.04	10.53

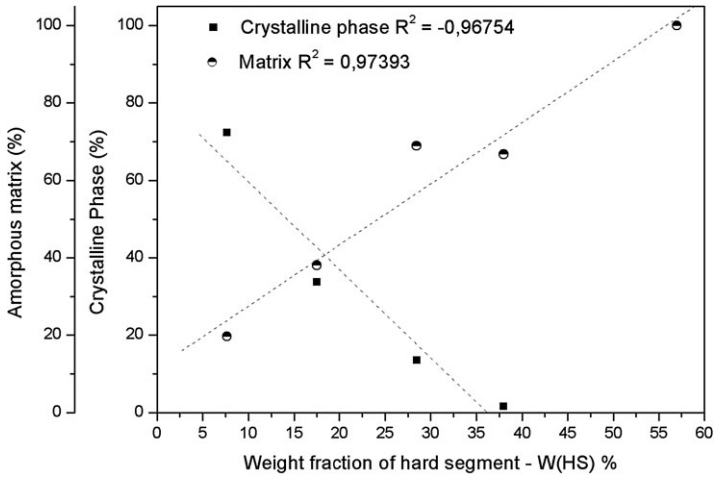

Figure 8.
Influence of hard segment content and $HBI^{(\%)}_{(C=O)}$ on the multiphase structure of polyurethane.

degree of phase separation or $100-DPM(\%)$ (Figure 7-a), SAXS's crystalline phase is reflected to α_{FTIR}, (Figure 7-b).

The $W(HS)$ influence on the microphase separation structure of PUs is illustrated in Figure 8. High segment contents promote phase mixture and decrease the chain mobility. Thus the soft segments are not able to align themselves to form crystals. Results in Table 4 shows that the amount of hard domains tend to decrease for samples having lower weight fractions of the hard segment as it is also observed by the $DPM(\%)$ values in Table 2.

Conclusion

Polyurethane with multiphase structure including: amorphous matrix, hard domains and crystals were produced by altering the hard segment content. The multi-phase structure of PUs was a result of the repulsive interaction between hard and soft segment. It was observed a relationship between hard segment content and phase mixture. High hard segment contents promoted phase mixture restricting segmental motion as a result, the soft segments were not able to align themselves to form crystals. SAXS results may be used to estimate the nano-morphology of segmented PUs. SAXS and FTIR results showed a good correlation. SAXS results described the degree of phase mixture and the crystallinity index.

Acknowledgements: The authors acknowledge the financial support from the following institutions: National Council for Scientific and Technological Development (CNPq), a foundation linked to the Ministry of Science and Technol-

ogy (MCT) of the Brazilian Government; the State of Minas Gerais Research Foundation (FAPEMIG); and the National Synchrotron Light Laboratory (LNLS-Brazil) for the use of the SAXS beamline facilities.

Y. Li, T. Gao, J. Liu, K. Linliu, C. R. Desper, B. Chu

[1] K. Nakamae, T. Nishino, S. Asaoka, Sudaryanto, *Int. J. Adhes. Adhes.* **1999**, *19*, 345.
[2] G. Pompe, A. Pohlers, P. Pötschke, J. Pionteck, *Polymer* **1998**, *39*, 5147.
[3] J. R. Lin, L. W. Chen, *J. Appl. Polym. Sci.* **1998**, *69*, 1563.
[4] Y. Li, T. Gao, J. Liu, K. Linliu, C. R. Desper, B. Chu, *Macromolecules* **1992**, *25*, 7365.
[5] I. M. Pereira, S. Carvalho, M. M. Pereira, M. F. Leite, R. L. Oréfice, *J. Appl. Polym. Sci.* **2009**, *114*, 254.
[6] I. W. Cheong, H. C. Kong, J. H. An, J. H. Kim, *J. Polym. Sci., Part A: Polym. Chem.* **2004**, *42*, 4353.
[7] Y. Liu, C. Pan, *Eur. Polym. J.* **1998**, *34*, 621.
[8] J. W. Cho, S. H. Lee, *Eur. Polym. J.* **2004**, *40*, 1343.
[9] E. Ayres, R. L. Oréfice, M. I. Yoshida, *Eur. Polym. J.* **2007**, *43*, 3510.
[10] H. Bao, Z. Zhang, S. Ying, *Polymer* **1996**, *37*(13), 2751.
[11] S. Wang, Y. Zhang, W. Ren, Y. Zhang, H. Lin, *Polym. Test.* **2005**, *24*, 766.
[12] Y. J. Li, W. X. Kang, J. O. Stoffer, et al. *Macromolecules* **1994**, *27*(2), 612.
[13] I. M. Pereira, R. L. Oréfice, *J. Mater. Sci.* **2010**, *45*, 511.

